

Stress analysis of a two-phase composite having a negative-stiffness inclusion in two dimensions

Yun-Che Wang[†] and Chi-Ching Ko

Engineering Materials Program, Department of Civil Engineering, Center for Micro/Nano Science and Technology, National Cheng Kung University, 1 University Avenue, Tainan, Taiwan 70101

(Received August 2, 2009, Accepted August 30, 2009)

Abstract. Recent development in composites containing phase-transforming particles, such as vanadium dioxide or barium titanate, reveals the overall stiffness and viscoelastic damping of the composites may be unbounded (Lakes *et al.* 2001, Jaglinski *et al.* 2007). Negative stiffness is induced from phase transformation predicted by the Landau phase transformation theory. Although this unbounded phenomenon is theoretically supported with the composite homogenization theory, detailed stress analyses of the composites are still lacking. In this work, we analyze the stress distribution of the Hashin-Shtrikman (HS) composite and its two-dimensional variant, namely a circular inclusion in a square plate, under the assumption that the Young's modulus of the inclusion is negative. Assumption of negative stiffness is *a priori* in the present analysis. For stress analysis, a closed form solution for the HS model and finite element solutions for the 2D composite are presented. A static loading condition is adopted to estimate the effective modulus of the composites by the ratio of stress to average strain on the loading edges. It is found that the interfacial stresses between the circular inclusion and matrix increase dramatically when the negative stiffness is so tuned that overall stiffness is unbounded. Furthermore, it is found that stress distributions in the inclusion are not uniform, contrary to Eshelby's theorem, which states, for two-phase, infinite composites, the inclusion's stress distribution is uniform when the shape of the inclusion has higher symmetry than an ellipse. The stability of the composites is discussed from the viewpoint of deterioration of perfect interface conditions due to excessive interfacial stresses.

Keywords: elasticity; composite; negative stiffness; interfacial stress; Eshelby's uniformity theory.

1. Introduction

In recent years, negative stiffness induced effective stiffness and damping anomalies have been studied experimentally (Lakes 2001, Lakes *et al.* 2001, Jaglinski *et al.* 2007) and theoretically (Lakes 2001, Wang and Lakes 2001, Lakes and Drugan 2002) to understand the phenomena. The negative stiffness is obtainable through different processes. In structural mechanics, negative stiffness is obtainable through post-buckling processes (Thompson 1982). In solid materials, the Landau phenomenological theory on phase transformation predicts negative curvature in system free energy, i.e., negative stiffness, in the vicinity of phase transitions (Falk 1980). Drastic enhancements in elastic modulus and linear viscoelastic damping of the negative-stiffness composites are the

[†] Professor, Corresponding author, E-mail: yunche@mail.ncku.edu.tw

driving force of continuing research in this field. In addition, particularly reported in Wang and Lakes (2001), unbounded increases and decreases in coupled-field properties, such as pyroelectricity and piezoelectricity, are predicted based on the composite homogenization theory. These composites are often called extreme composites due to their enhanced physical properties.

Recent theoretical studies have shown that negative stiffness inclusions can be stabilized in a positive-stiffness coating (Drugan 2007, Kochmann and Drugan 2009) in accordance to elasticity theory, but the extreme properties are not analyzed with stability. Mathematical proof on the positive eigenvalues in negative shear modulus materials can be found in Ernst (2004), showing the possibility of positive wave speeds in elastic medium under the negative modulus assumptions. Stability discussions based on thermodynamics and energy arguments can be found in Shang and Lakes (2007), Lakes and Wojciechowski (2008). These references provide foundations in assuming negative stiffness in mechanics analysis. Negative stiffness does not imply the existence of perpetual machines, because it is a structural effect. Extreme properties and stability analysis based on discrete mechanical models can be found in Wang and Lakes (2004), Wang (2007), and references therein. Molecular simulations in polymer systems at small scales have shown the presence of negative stiffness (Yoshimoto *et al.* 2004).

Recent experimental results on using barium titanate as inclusions in tin matrix to show composites may exhibit viscoelastic stiffness greater than that of diamond (Jaglinski *et al.* 2007). However, the anomalous stiffness and damping disappeared after some cycles of phase transition in barium titanate. More recent experimental results on detecting negative stiffness effects in carbon nanotubes have been reported in Yap *et al.* (2007, 2008).

In the present analysis, two-dimensional plane-stress elasticity problem is analyzed to study the effects of negative-stiffness inclusion in a square plate. Our analysis adopts the finite element methods to carry out numerical calculations of the corresponding elasticity problem. Although stability of systems of this kind is of great interest and importance, we focus ourselves on the stress analysis in the composite to understand the irreversible properties found in the experiment (Jaglinski *et al.* 2007), and infer the loss of stability when interfacial stresses are abnormally large to the strength of perfect bonding between the inclusion and matrix.

2. Linear elasticity

To solve the two-dimensional elasticity problem with a circular inclusion in a square plate, as shown in Fig. 1 for the quarter of the physical problem because of symmetry, the finite element solver (COMSOL Multiphysics) was adopted for numerical calculations. Starting from the relationships between strain ($\varepsilon_{\alpha\beta}$) and displacement (u_α or \mathbf{u}) in linear elasticity, shown in Eq. (1), one can obtain the Navier's equation for the numerical calculations as follows. The subscripts α and β range from 1 to 2. Vectors are denoted with bold-face type characters.

$$\varepsilon_{\alpha\beta} = \frac{1}{2} \left(\frac{\partial u_\alpha}{\partial x_\beta} + \frac{\partial u_\beta}{\partial x_\alpha} \right) \quad (1)$$

The balance law from the Newton's second law can be expressed as below in terms of stresses and displacements.

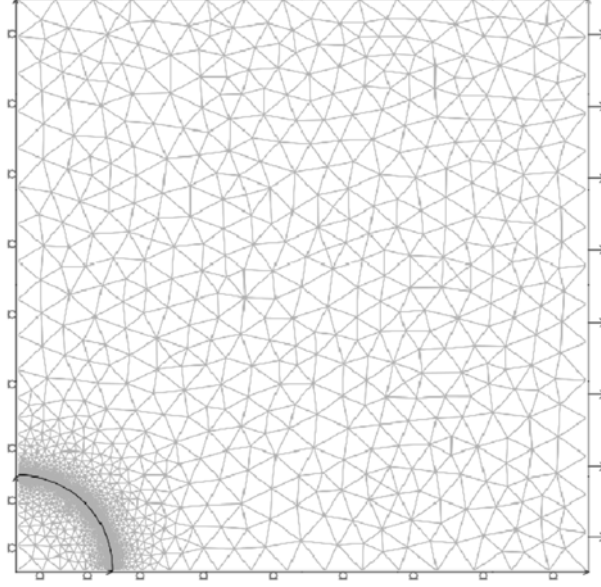


Fig. 1 Finite element model of the quarter of the physical problem. (a) displacement and loading boundary conditions and (b) the meshes used in the numerical calculations. The origin of the Cartesian coordinate is at the lower left corner, and the x-axis points toward right and the y-axis upward. Assume the radius of the circular inclusion $a = 1$ m, and the half-width of the square plate is $b = 6$ m. Corresponding volume fraction is 2.18%. Units may be scalable down to nano scales since there are no length parameters in elasticity analysis. The number of meshes was about 5000, and triangular Lagrange elements were adopted

$$\frac{\partial \sigma_{\alpha\beta}}{\partial x_{\beta}} + \rho b_{\alpha} = \rho \ddot{u}_{\alpha} \quad (2)$$

Here b_{α} or \mathbf{b} represents the specific body force, and ρ the density of the body. The constitutive relationships for linear elastic responses are

$$\varepsilon_{\alpha\beta} = S_{\alpha\beta\gamma\delta} \sigma_{\gamma\delta} \quad (3)$$

$$S_{\alpha\beta\gamma\delta} = \frac{1}{4\mu} (\delta_{\alpha\gamma} \delta_{\beta\delta} + \delta_{\alpha\delta} \delta_{\beta\gamma}) - \frac{\nu}{2\mu(1+\nu)} \delta_{\alpha\beta} \delta_{\gamma\delta} \quad (4)$$

The symbol $S_{\alpha\beta\gamma\delta}$ represents the fourth-order identity tensor. The Navier's equation can be conventionally expressed as in Eq. (5), after combining the strain-displacement relationships (1), balance law (2) and constitutive relationships (3), provided with the Lamé constants being independent on space coordinates.

$$\mu \nabla^2 \mathbf{u} + (\lambda + \mu) \nabla (\nabla \cdot \mathbf{u}) + \rho \mathbf{b} = \rho \ddot{\mathbf{u}} \quad (5)$$

By applying the divergence operation on the both sides of the above equation, the Navier's equation can be re-written as

$$\mu \nabla^2 (\nabla \cdot \mathbf{u}) + (\lambda + \mu) \nabla \cdot \nabla (\nabla \cdot \mathbf{u}) + \rho \nabla \cdot \mathbf{b} = \rho \nabla \cdot \ddot{\mathbf{u}} \quad (6)$$

Further manipulation results in

$$\nabla \bullet [c \nabla (\nabla \bullet \mathbf{u}) + \rho \mathbf{b}] = \nabla \bullet (\rho \ddot{\mathbf{u}}) \quad (7)$$

and hence

$$c \nabla \bullet (\nabla \mathbf{u}) + \rho \mathbf{b} = \rho \ddot{\mathbf{u}} \quad (8)$$

where $c = \lambda + 2\mu$. For general anisotropic and heterogeneous materials, the Navier's equations can be expressed as follows.

$$\nabla \bullet (C : \nabla \mathbf{u}) + \rho \mathbf{b} = \rho \ddot{\mathbf{u}} \quad (9)$$

Here C is a fourth-order tensor, and the symbol, $:$, indicates the inner product between a fourth-order and second-order tensor. In the present analysis, the body force \mathbf{b} is neglected and only quasi-static responses are studied. Therefore, the Navier's equation takes the form as below.

$$\nabla \bullet (C : \nabla \mathbf{u}) = \mathbf{0} \quad (10)$$

To numerically solve the governing equation, Eq. (10), a weak-form solution (Shi and Tang 2008) technique combining with linear Lagrange finite element was adopted.

Boundary conditions of the two-dimension elasticity problem must be provided by prescribing the loading conditions on the 'natural' boundaries, or prescribing the displacement conditions on the 'essential' boundaries. The union of natural and essential boundaries form the entire boundary of the body. In the present analysis, the plate is subjected to uniform loading on the left and right edges. Displacement boundary conditions are not prescribed. Rigid body motion has been suppressed.

For a composite system, uniformly applied loading at the boundaries do not ensure uniform strain distributions correspondingly. To estimate the effective modulus of the composite under the loading condition (uniform applied stress on the left and right edges), we adopt the averaged strain,

$$\bar{\varepsilon} = \frac{2}{l} \int_0^{l/2} \varepsilon(y) dy \quad (11)$$

and define the ratio of the applied stress to the average strain as the effective Young's modulus of the composite. The strain energy of the system may be calculated as follows.

$$U = \int_{\Omega} \mu \varepsilon_{\alpha\beta} \varepsilon_{\alpha\beta} + \frac{\lambda}{2} (\varepsilon_{\gamma\gamma})^2 d\Omega \quad (12)$$

where Ω denotes the domain of the physical problem, and the integration must be performed region by region for the composite. To estimate the interfacial stresses between the inclusion and matrix, the von Mises stress is adopted as a measure of effective stress, and defined as follows.

$$\sigma_{eff} = \sqrt{3J_2} \quad (13)$$

$$J_2 = \frac{1}{6} [(\sigma_1 - \sigma_2)^2 + (\sigma_2 - \sigma_3)^2 + (\sigma_3 - \sigma_1)^2] \quad (14)$$

3. Composite theory

For the three-dimensional Hashin-Shtrikman coated sphere, the stresses in the inclusion

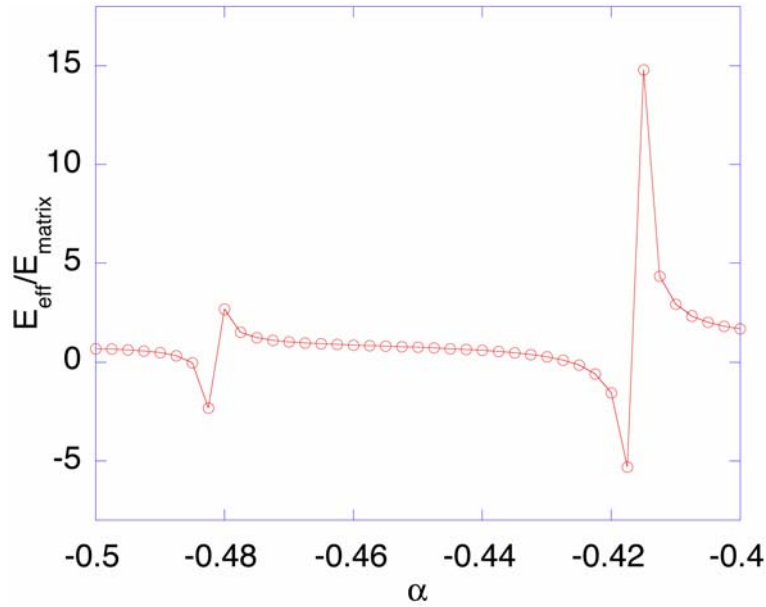


Fig. 2 Normalized effective Young's modulus ($E_{\text{eff}}/E_{\text{matrix}}$) vs. tuning parameter α ($\alpha = E_{\text{inc}}/E_{\text{matrix}}$)

(superscript or subscript i) and matrix (superscript or subscript m) may be calculated as follows.

$$\sigma_{rr}^i = \sigma_{\phi\phi}^i = \sigma_{\theta\theta}^i = \sigma_{rr}^m = \frac{k_i(3k_m + 4\mu_m)}{4c\mu_m(k_i - k_m) + k_m(3k_i + 4\mu_m)} \quad (15)$$

$$\sigma_{\phi\phi}^m = \sigma_{\theta\theta}^m = \frac{3k_i k_m - 4k_i \mu_m + 8k_m \mu_m}{4c\mu_m(k_i - k_m) + k_m(3k_i + 4\mu_m)} \quad (16)$$

Here k , m and c represent, respectively, the bulk modulus, shear modulus and volume fraction of the inclusion, i.e., $c = (a/b)^3$, and a is the radius of the inner sphere and b is the outer sphere. From the above equations, it can be seen that with suitable inclusion modulus the interfacial stresses may become singular.

4. Results and discussion

The enhancement due to negative-stiffness inclusion on effective Young's modulus is shown in Fig. 2. The effective Young's modulus was calculated by taking the ratio of applied uniform load (1 Pa) to the averaged strain (see Eq. (11)) on the loading edge. The Young's modulus of the matrix is assumed to be 200 GPa. Throughout the present analysis, the Poisson ratio of both the inclusion and matrix is assumed to be 0.3. Negative Young's modulus with positive Poisson ratio implies negative shear modulus ($G = E / 2(1 + \nu)$) for isotropic materials. Negative shear modulus may be allowable in isotropic materials with suitable boundary conditions (Ernst 2004), and requires further investigation in composite systems. The magnitude of the enhancement is beyond the prediction of conventional composite theory, assuming both phases having positive stiffness. Remark that the

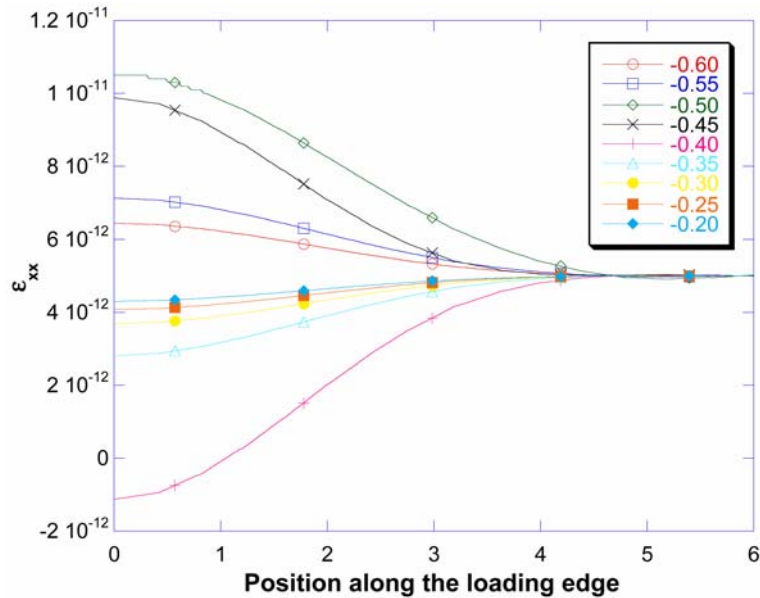


Fig. 3 Strain distribution along the loading edge. The strain scale is small due to the applied stress being 1 Pa. The position along the loading edge measures from the bottom edge of Fig. 1 upwards (i.e. along the y-axis). The extreme small numbers on the vertical axis are due to small applied load and large Young's modulus to ensure the system is in the regime of linear elasticity

rules of mixture cannot predict overall properties greater or smaller those of the mixture's constituents. Two stiffness peaks are observed due to different modes, one corresponding to the bulk response (smaller $|\alpha|$) and the other the shear response (larger $|\alpha|$). The rationale for this correspondence is due to the mechanical behavior of uniaxial tension can be considered as the superposition of two orthogonal deformation modes, dilatation and shear. Hence, two stiffness peaks can be observed from uniaxial loading. This result is consistent with previous studies on discrete composite systems (Wang 2007, Wang *et al.* 2007). The degree of instability for the shear mode is greater than that for the bulk mode. Therefore, the shear mode requires larger amount of negative stiffness (i.e. the absolute value of α is larger). The more negative stiffness is used in the system, the higher divergent rates for instability (Wang and Lakes 2004).

Fig. 3 shows the strain distributions on the loading edge along the y-axis for different inclusion moduli. It is known that due to the inhomogeneity from the mismatch between the inclusion and matrix, the strain distributions are non-uniform. When the inclusion's modulus is negative, the trends of strain distributions differ from expectation. First, when α , defined as the ratio of inclusion's Young's modulus to the Young's modulus of the matrix, decreases from -0.2 to about -0.43 (where the first stiffness peak occurs), the strains become smaller near the center of the loading edge. It may become negative ($\alpha = -0.4$), indicating the center region of the loading edge deforms in the opposite direction of the applied load. When α decreases from -0.5 to -0.6, the strains also become smaller, but the distributions differ from α being in the -0.2 to -0.43 region. This phenomenon indicates negative stiffness may exhibit singularity-like behavior. In other words, the strain distributions are following completely different trends before and after the first stiffness peak. Due to the strong effects on the strains on the loading edges, the effective approaches to study

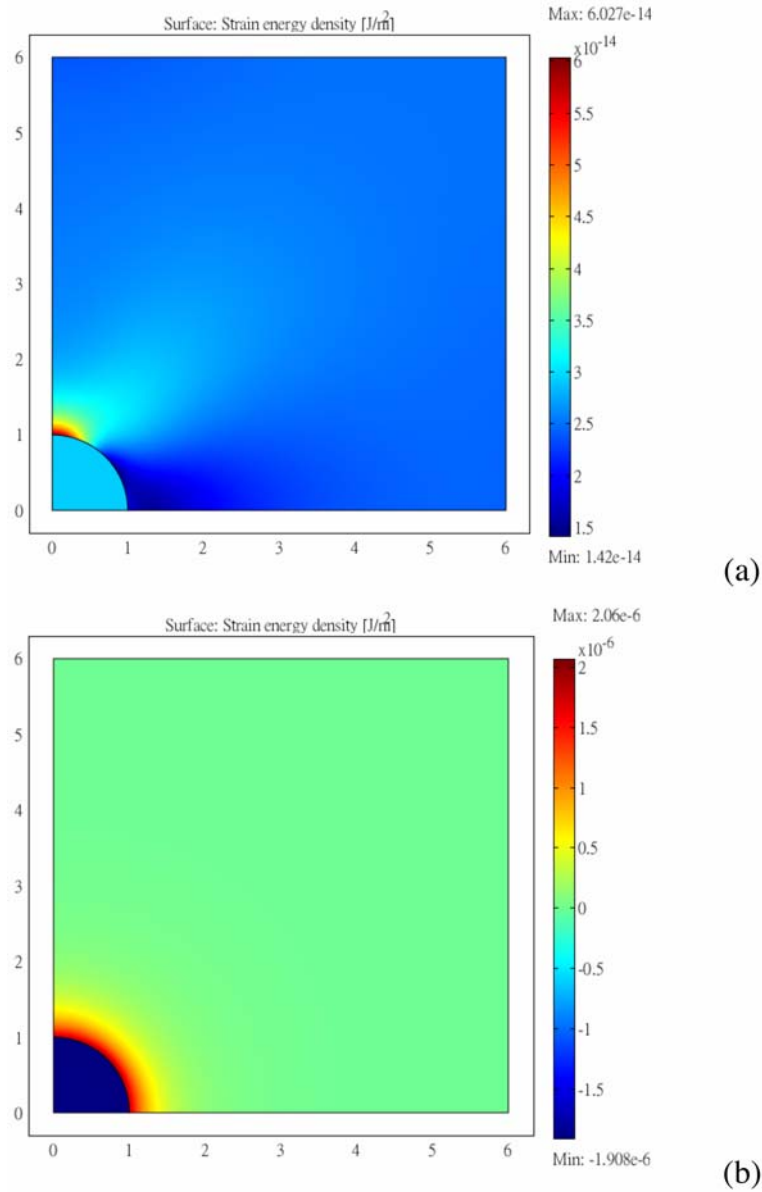


Fig. 4 (a) Strain energy density for the positive-stiffness composite, (b) strain energy density for the negative-stiffness composite

composites may require further refinements. Remark that the magnitude of the strains is extremely small due to the small applied load and the Young's modulus of steel.

The results of strain energy density calculation are shown in Figs. 4 (a) and (b) for positive- and negative-stiffness composites, respectively. As expected, the stress concentration in the positive-stiffness composite is in a portion of the inclusion, and all energy density is positive. However, the negative-stiffness composites show that the matrix does not store elastic energy, and most of the elastic energy occurs near the interface between the inclusion and the matrix. Inside the inclusion,

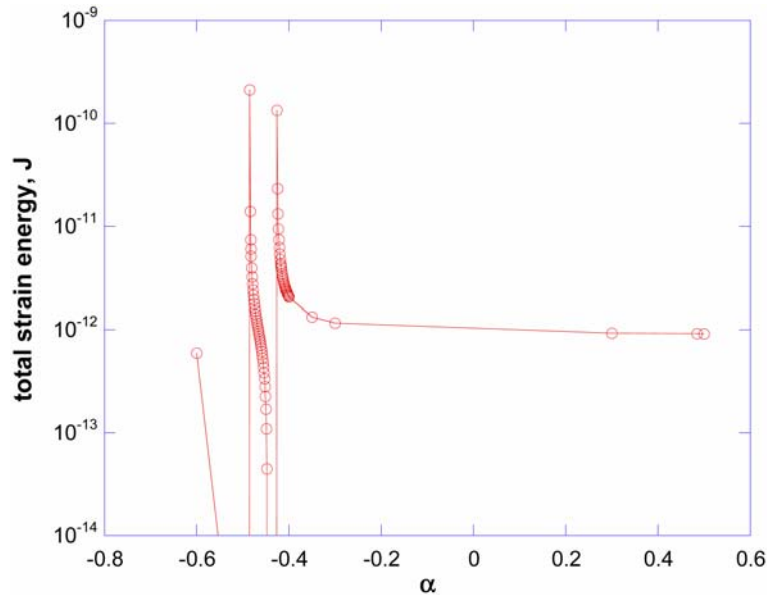


Fig. 5 Total strain energy of the negative-stiffness composite vs. the strength of negative stiffness in the inclusion

the energy density is negative, which is not stable based on the energy-based stability theorems. However, if one looks at the total strain energy of the composite system, as shown in Fig. 5 (vertical axis on the log scale), the energy accumulates rapidly near the α value that corresponds to the extreme properties. In some regions, the total strain energy is negative. It is known that the total strain energy cannot be used as an indicator to describe stability (Thompson 1982, Hill 1957). Point-wise stability requires strain energy density to be positive locally. However, total strain energy, the sum of strain energy density in the volume of the domain, only provides global information of the system. The coincidence between the total energy peaks and stiffness peaks and Lyapunov stability analysis on other systems show that the interplay between the negative-stiffness inclusion and matrix may provide stronger stability that predicted by the point-wise energy-based stability theory. Furthermore, the difference in magnitudes of the positive- and negative- composites is large, indicating the strong elastic interaction in the composites.

The von Mises stresses in the inclusion are shown in Fig. 6. For positive-stiffness inclusions ($\alpha = 0.5$), the Eshelby's uniformity theorem holds if the matrix is large enough, as shown in Fig. 6 (a). Three plate sizes are calculated, as indicated $a/b = 1/2, 1/3$ and $1/6$, where a is the radius of the circular inclusion and b the half width of the plate. The a/b ratio is considered as linear volume fraction of the composite. In Fig. 6 (b), the a/b ratio is fixed, equal to $1/6$, and von Mises stresses in the inclusion are calculated for various α . The magnitudes of the von Mises stresses are much larger than the positive-stiffness case, indicating the inclusion is highly stresses when its modulus is negative. In physical reality, the large stress may cause the inclusion plastically yield or fracture.

In Fig. 7, the traction along the x-axis at the position on the interface measured from the horizontal axis in terms of θ is plotted. It can be seen that when $\alpha = 0.5$, the traction is small due to applied load is 1 Pa. However, for negative α , the traction increases significantly, indicating the interface suffers tremendous stress. The trend of the traction increases and the value of a appears to

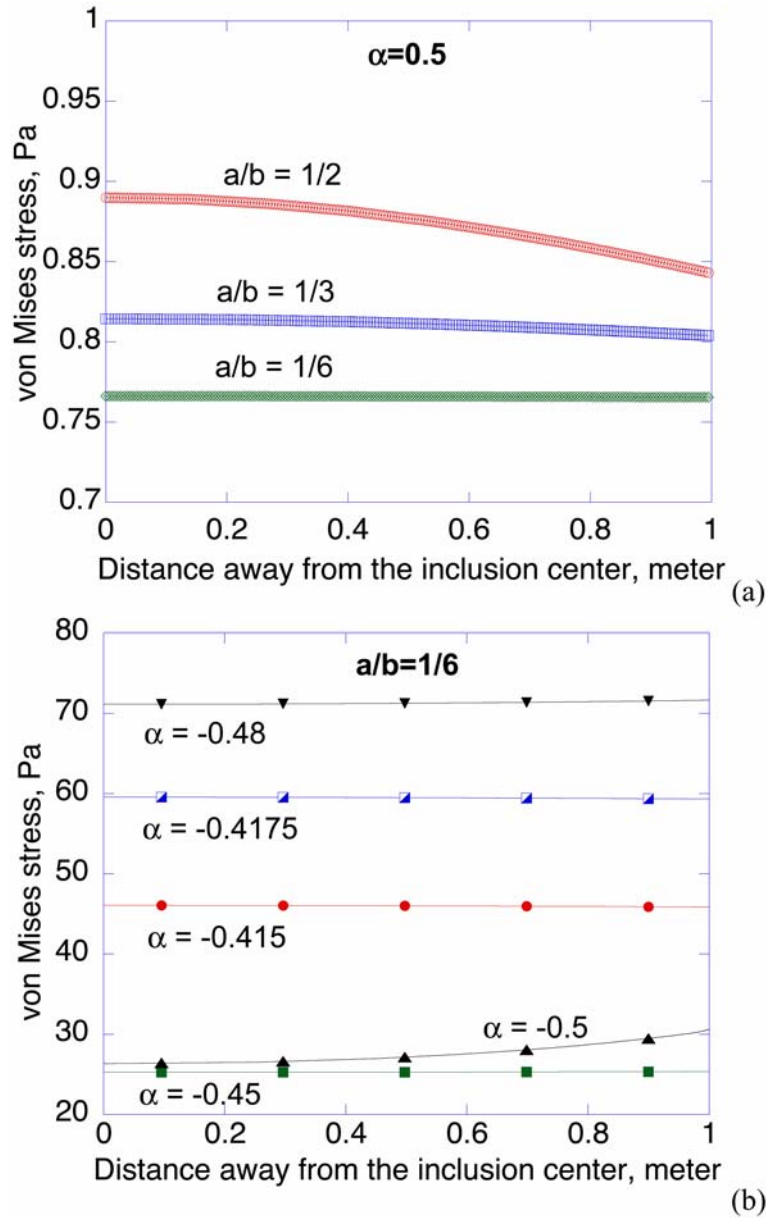


Fig. 6 The von Mises stress in the inclusion along the x-axis for positive-stiffness inclusion (a), and for negative -stiffness inclusion (b) with linear volume fraction (a/b) being $1/6$. Negative stiffness may change Eshelby's uniformity results

be affected by the singularity in the system stiffness. When α is very close to that causes the stiffness peak ($\alpha = -0.485$), the traction increase unboundedly. This same phenomenon is observed in the strain distribution, as shown in Fig. 3. Furthermore, from the von Mises stress calculation, the negative-stiffness inclusion causes large interfacial stress, reaching singular, on the inclusion-matrix interface, as shown in Fig. 8. This calculated results can be justified from the analytical results

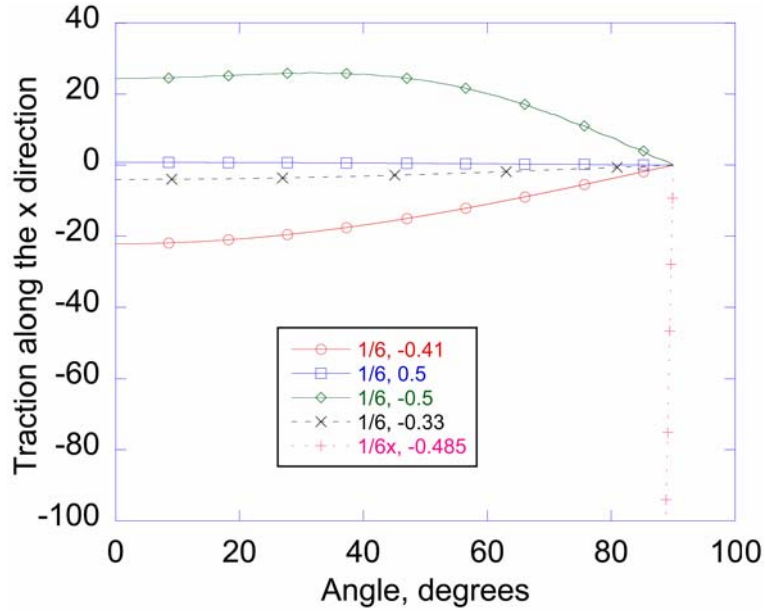


Fig. 7 Traction along the circular edge of the inclusion in the first quadrant. The $\theta=0^\circ$ indicates the interface point on the x-axis, and $\theta=90^\circ$ the interface point on the y-axis. Vertical axis is in units of Newton

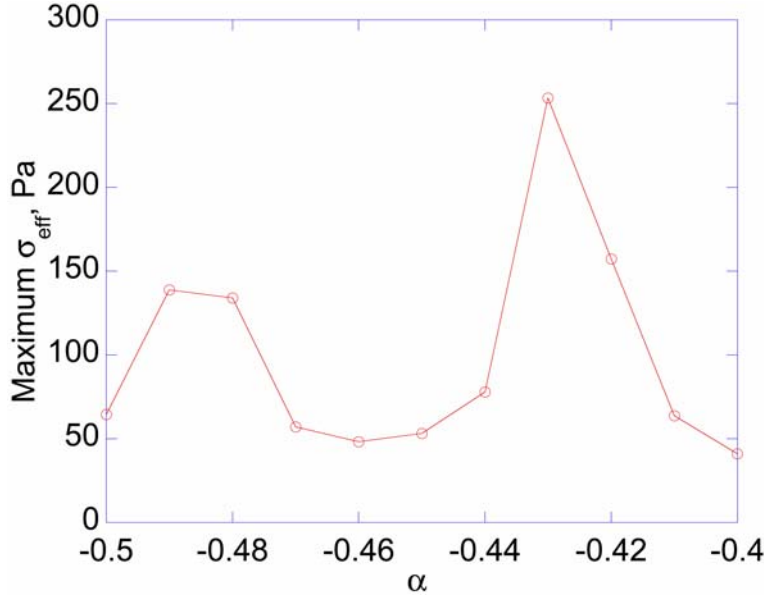


Fig. 8 Maximum von Mises stress (σ_{eff}) at the inclusion-matrix interface for various α . Applied load is 1 Pa

shown in Eqs. (15) and (16). The two peaks in effective stresses correspond the stiffness peaks in Fig. 2. Such high interfacial stresses may be responsible for irreversible properties found in the experiment (Jaglinski *et al.* 2007).

5. Conclusions

Under plane stress assumptions, the two-dimensional elasticity problem of a square plate with a circular inclusions demonstrates the negative-stiffness inclusion increases the overall Young's modulus of the composite beyond the prediction of the conventional composite theory. For negative-stiffness inclusion, the inclusion-matrix interfacial stresses and interior stresses in the inclusion are much larger than the case with positive-stiffness inclusion. Eshelby's uniformity theorem may hold for negative stiffness away from stiffness peak regions. Near the stiffness peaks, the stress and strain distributions are highly nonlocal.

Acknowledgements

The authors are grateful for a grant from Taiwan National Science Council (NSC 97-2221-E-006-143 and NSC 98-2221-E-006-131-MY3).

References

- Lakes, R.S. (2001), "Extreme damping in compliant composites with a negative-stiffness phase", *Philos. Mag. Lett.*, **81**(2), 95-100.
- Lakes, R.S., Lee, T., Bersie, A. and Wang, Y.C. (2001), "Extreme damping in composite materials with negative-stiffness inclusions", *Nature*, **410**, 565-567.
- Jaglinski, T., Kochmann, D., Stone, D. and Lakes, R.S. (2007), "Composite materials with viscoelastic stiffness greater than diamond", *Science*, **315**, 620-622.
- Lakes, R.S. (2001), "Extreme damping in composite materials with a negative stiffness phase", *Phys. Rev. Lett.*, **86**, 2897-2900.
- Wang, Y.C. and Lakes, R.S. (2001), "Extreme thermal expansion, piezoelectricity, and other coupled field properties in composites with a negative stiffness phase", *J. Appl. Phys.*, **90**, 6458.
- Lakes, R.S. and Drugan, W.J. (2002), "Dramatically stiffer elastic composite materials due to a negative stiffness phase", *J. Mech. Phys. Solids*, **50**, 979-1009.
- Thompson, J.M.T. (1982), "'Paradoxical' mechanics under fluid flow", *Nature*, **296**, 135-137.
- Falk, F. (1980), "Model free energy, mechanics and thermodynamics of shape memory alloys", *Acta Metall.*, **28**, 1773-1780.
- Drugan, W.J. (2007), "Elastic composite materials having a negative stiffness phase can be stable", *Phys. Rev. Lett.*, **98**, 055502.
- Kochmann, D.M. and Drugan, W.J. (2009), "Dynamic stability analysis of an elastic composite material having a negative-stiffness phase", *J. Mech. Phys. Solids*, **57**, 1122-1138.
- Ernst, E. (2004), "On the Existence of Positive Eigenvalues for the Isotropic Linear Elasticity System with Negative Shear Modulus", *Commun. Part. Diff. Eq.*, **29**, 1745-1753.
- Shang, X.C. and Lakes, R.S. (2007), "Stability of elastic material with negative stiffness and negative Poisson's ratio", *Phys. Status Solidi. B.*, **244**, 1008-1026.
- Lakes, R.S. and Wojciechowski, K.W. (2008), "Negative compressibility, negative Poisson's ratio, and stability", *Phys. Status Solidi. B.*, **245**, 545-551.
- Wang, Y.C. and Lakes, R.S. (2004), "Extreme stiffness systems due to negative stiffness elements", *Am. J. Phys.*, **72**, 40-50.
- Wang, Y.C. (2007), "Influences of negative stiffness on a two-dimensional hexagonal lattice cell", *Philos. Mag.*, **87**, 3671-3688.
- Yoshimoto, K., Jain, T.S., Van Workum, K., Nealey, P.F. and de Pablo, J.J. (2004), "Mechanical heterogeneities

- in model polymer glasses at small length scales”, *Phys. Rev. Lett.*, **93**, 175501.
- Yap, H.W., Lakes, R.S. and Carpick, R.W. (2007), “Mechanical instabilities of individual multiwalled carbon nanotubes under cyclic axial compression”, *Nano Lett.*, **7**, 1149-1154.
- Yap, H.W., Lakes, R.S. and Carpick, R.W. (2008), “Negative stiffness and enhanced damping of individual multiwalled carbon nanotubes”, *Phys. Rev. B.*, **77**, 045423.
- Shi, G and Tang, L. (2008), “Weak forms of generalized governing equations in theory of elasticity”, *Interact. Multi. Mech.*, **1**(3), 329-337.
- Wang, Y.C., Swadener, J.G. and Lakes, R.S. (2007), “Anomalies in stiffness and damping of a 2D discrete viscoelastic system due to negative stiffness components”, *Thin Solid Films*, **515**, 3171-3178.
- Thompson, J.M.T. (1982), “‘Paradoxical’ mechanics under fluid flow”, *Nature*, **296**, 135-137.
- Hill, R. (1957), “On uniqueness and stability in the theory of finite elastic strain”, *J. Mech. Phys. Solids*, **5**, 229-241.